Supplemental Digital Content

Sufentanil plasma concentrations were analyzed by non-linear mixed-effects modeling using NONMEM (Version 7.3.0, ICON Development solutions, Hanover, MD). The first-order conditional estimation method with interaction (FOCEI) was used throughout the analysis. Interindividual variability was assumed to follow a log-normal distribution. For i^{th} individual:

$$\theta_i = \theta_{POP} \cdot e^{\eta_i}$$

in which θ_i is the individual value of the parameter θ, θ_{POP} is the population value of this parameter, and η_i is a random variable with mean zero and variance ω_η^2. For the intra-individual variability describing the residual errors, a proportional error model was used:

$$c_{ij} = cp_{ij} + cp_{ij} \cdot \varepsilon_{ij}$$

in which c_{ij} is the j^{th} measured concentration of the i^{th} individual, cp_{ij} is the corresponding predicted concentration and ε_{ij} is a random variable with mean zero and variance σ^2.

Model Development

Modeling was performed sequentially: A basic structural model was determined first fitting two- and three-compartment models with first order elimination to the data. Estimated parameters were volumes of distribution, and elimination and intercompartmental clearances. The individual Bayesian estimates of the pharmacokinetic parameters were plotted independently against the weight and against the individual median value of the cardiac output. We assessed η-shrinkage to assure the informative value of the individual Bayesian estimates. Linear regression analysis was used as a first test for covariate effects. Subsequently, selected covariates were incorporated to the basic structural model using linear

relationships with centering on the median value of the covariate (*COV*) within the population:

$$\theta_{POP} = \theta_{TV} \cdot (1 + \theta_{COV} \cdot \frac{COV - Median(COV)}{Median(COV)})$$

in which θ_{TV} is the typical value of the parameter and θ_{COV} quantifies the covariate effect. The covariate parameter was included in the model, if the decrease in the NONMEM objective function value (ΔOFV) was at least 3.84 ($P < 0.05$) and if the 95% confidence interval of the additional parameter did not include zero. Subsequently, backward deletion analysis was performed and each covariate effect was tested again for significance by fixing the corresponding parameter $\theta_{COV} = 0$. This time, a more conservative significance level of $P < 0.01$ was used, which corresponds to an increase in ΔOFV of 6.6 for one degree of freedom.

Model Evaluation and Validation

Criteria for goodness of fit were the visual inspection of the following plots: : (i) measured concentrations vs. population predictions and vs. individual predictions, (ii) conditional weighted residuals vs. time and vs. population predictions, and (iii) ratio of measured to predicted concentration vs. time. Additionally, we calculated for each sample the prediction error PE_{ij}:

$$PE_{ij} = \frac{Cm_{ij} - Cp_{ij}}{Cp_{ij}} \cdot 100\%$$

where Cm_{ij} and Cp_{ij} are the i^{th} measured and predicted concentration of the j^{th} individual, respectively. Prediction errors were determined for individual and population predictions, and goodness of fit was assessed by the median prediction error MDPE=median(PE_{ij}) and the median absolute prediction error MDAPE=median(|PE_{ij}|).

The reliability of the pharmacokinetic parameter estimates was further assessed by likelihood profiling. For this purpose, the parameter to be assessed was fixed at particular values around its final population estimate and the corresponding OFV was determined. The plot of the OFV vs. the parameter values helps to identify problems with parameter estimability.

Using the final model and the original data set, bootstrap resampling analysis with 1000 replicates (by subject with replacement) was conducted for validation of the model and to obtain nonparametric confidence intervals of the final population model parameters.

To test the predictive value of the final model on data that were not used for model building, we also performed a cross-validation. For this purpose, we constructed 7 test sets and 7 corresponding estimation sets. Each test set contained the data of three randomly selected animals; the corresponding estimation set contained the data of the remaining 17 animals. As the total number of studied animals was 20, the last test set contained only 2 animals and the last estimation set 18 animals. The random selection of the test animals was performed without replacement, so that each animal is contained only once in the test sets. Each test set contained one animal of each group, except the last test set, in which the two animals were from the normal and low cardiac output group. The final model was then fitted to each of the 7 estimation sets, and the prediction errors were estimated in the corresponding test set using the population parameter estimates obtained from the estimation set in this run.

Results

A two-compartment model fitted best the time profile of sufentanil concentrations (figure S1). Figure S2 depicts the sufentanil washout curves after the end of sufentanil infusion (please consider the alignment of the two animals whose sufentanil infusion lasted longer (figure S2A), and the differences in normalized washout curves between groups (figure S2B)). A three-compartment model could not be estimated reliably as indicated by the likelihood

profiles which showed no clear minimum for the volume of distribution of the third compartment. The η-shrinkage of the basic two-compartment model was less than 10% for all clearance and volumes, indicating sufficient informative value of the individual estimates. The linear regression analysis of the individual estimates showed a significant increase of all clearances and volumes with cardiac output, whereas age and weight did not show any effect on pharmacokinetic parameters. We therefore included cardiac output as covariate for all clearances and volumes of distribution, assuming a linear relationship as described above. When compared with the basic model without covariates, the inclusion of cardiac output for all pharmacokinetic parameters resulted in a significant improvement of fit (ΔOFV = 52.4). Backward deletion analysis confirmed the significance of the cardiac output effect, as the objective function increased by more than 10 if the cardiac output effect was removed from the model for any of the pharmacokinetic parameters (i.e., 25.7 for CL1, 14.2 for V1, 53.8 for CL2, 29.0 for V2).

The final pharmacokinetic two-compartment model is presented in the article. Quality of fit was good with low prediction errors, as indicated by a MDPE of 3.9% and a MDAPE of 21.2%, and relatively homogenous distributions of the residuals (figure S3). The likelihood profiles indicated reliable parameter estimations (figure S4). The inclusion of CO as a model covariate led to a distinct reduction in the interindividual variability of model parameters and improved the performance and predictive value of the model, as reflected by the coefficients of variation, the population prediction errors and the cross-validation results, respectively (data presented in the article).

Simulations

In addition to the simulations presented in the article, we also analyzed the impact of a hypothetical normalization of altered CO on dosing and context-sensitive decrement times.

Figure S5 shows the sufentanil infusion rates needed to maintain a constant sufentanil plasma concentration of 0.5 ng · ml^{-1} for 3 h when altered CO returns to normal within 15, 30, and 60 min after start of sufentanil infusion. The hypothetical CO normalization was simulated by a linear increase of CO from 3 to 5 $L \cdot min^{-1}$ and by a linear decrease of CO from 7 to 5 $L \cdot min^{-1}$ during the above-mentioned time periods. Infusion rates as for a constant CO of 5 $L \cdot min^{-1}$ were achieved in both cases within approximately 90 min after infusion start (figures S5A and S5B). In case of an initial CO of 3 $L \cdot min^{-1}$, the total sufentanil doses after 3 h of infusion were 126.5, 124.8 and 122.1 µg for a restoration of normal CO within 15, 30, and 60 min, respectively (figure S5C). In case of an initial CO of 7 $L \cdot min^{-1}$, the total sufentanil doses after 3 h of infusion were 130.5, 131.8 and 133.9 µg (figure S5D).

Further, we simulated 25%, 50% and 75% decrement times for the situation when altered CO returns to normal values after stop of sufentanil infusions for maintaining a plasma concentration of 0.5 ng · ml^{-1} for 30, 60, 120, and 180 min. Again, the hypothetical CO normalization was simulated by a linear increase of CO from 3 to 5 $L \cdot min^{-1}$ (figure S6) and by a linear decrease of CO from 7 to 5 $L \cdot min^{-1}$ (figure S7) within 15, 30, 60 min after infusion. As depicted in both figures, CO changes causes increased decrement times when related to the baseline decrement times with constant CO, i.e., 3 or 7 $L \cdot min^{-1}$. In case of a change in CO from 3 to 5 $L \cdot min^{-1}$, the decrement times were equal to or longer than those for a CO of 3 $L \cdot min^{-1}$, but shorter than those for a CO of 5 $L \cdot min^{-1}$. In case of a change in CO from 7 to 5 $L \cdot min^{-1}$, the decrement times were equal to or longer than those for a CO of 7 $L \cdot min^{-1}$, and longer than those for a constant CO of 5 $L \cdot min^{-1}$. These findings may be explained by CO induced changes in volumes of distribution and redistribution processes from peripheral to central compartment (figure S8). However, the simulation results should be interpreted cautiously as they are not supported by the present study design.

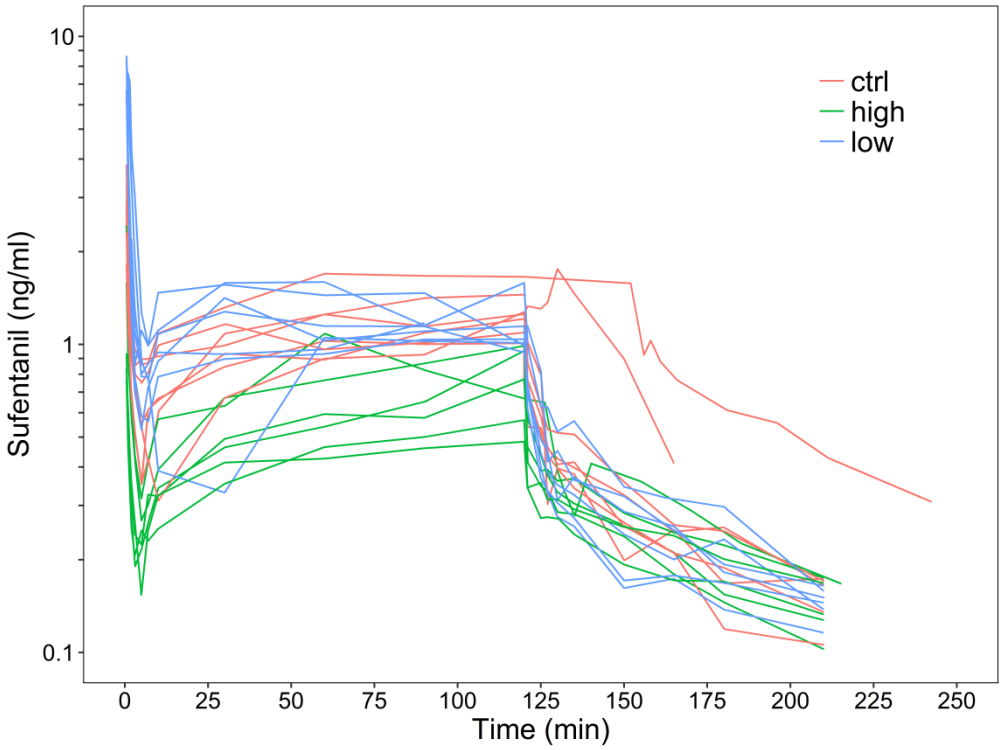

Figure S1: Time course of sufentanil plasma concentration in each animal. ctrl, control group; low, low cardiac output group; high, high output cardiac group.

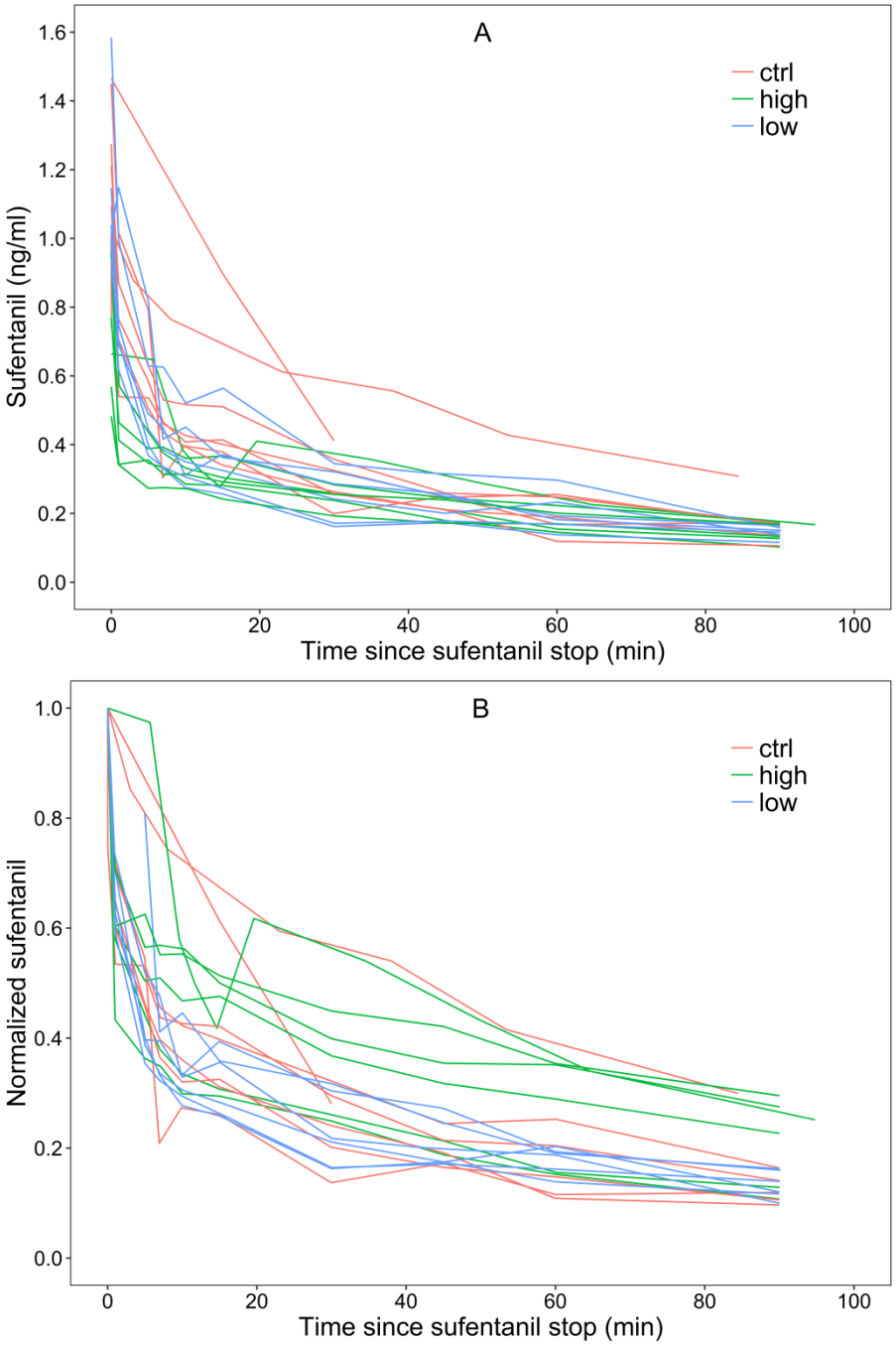

Figure S2: Time course of sufentanil plasma concentration in each animal after stop of sufentanil infusion. Panel A depicts the raw data, and panel B shows the sufentanil concentrations normalized to the concentration at the end of sufentanil infusion. ctrl, control group; low, low cardiac output group; high, high output cardiac group.

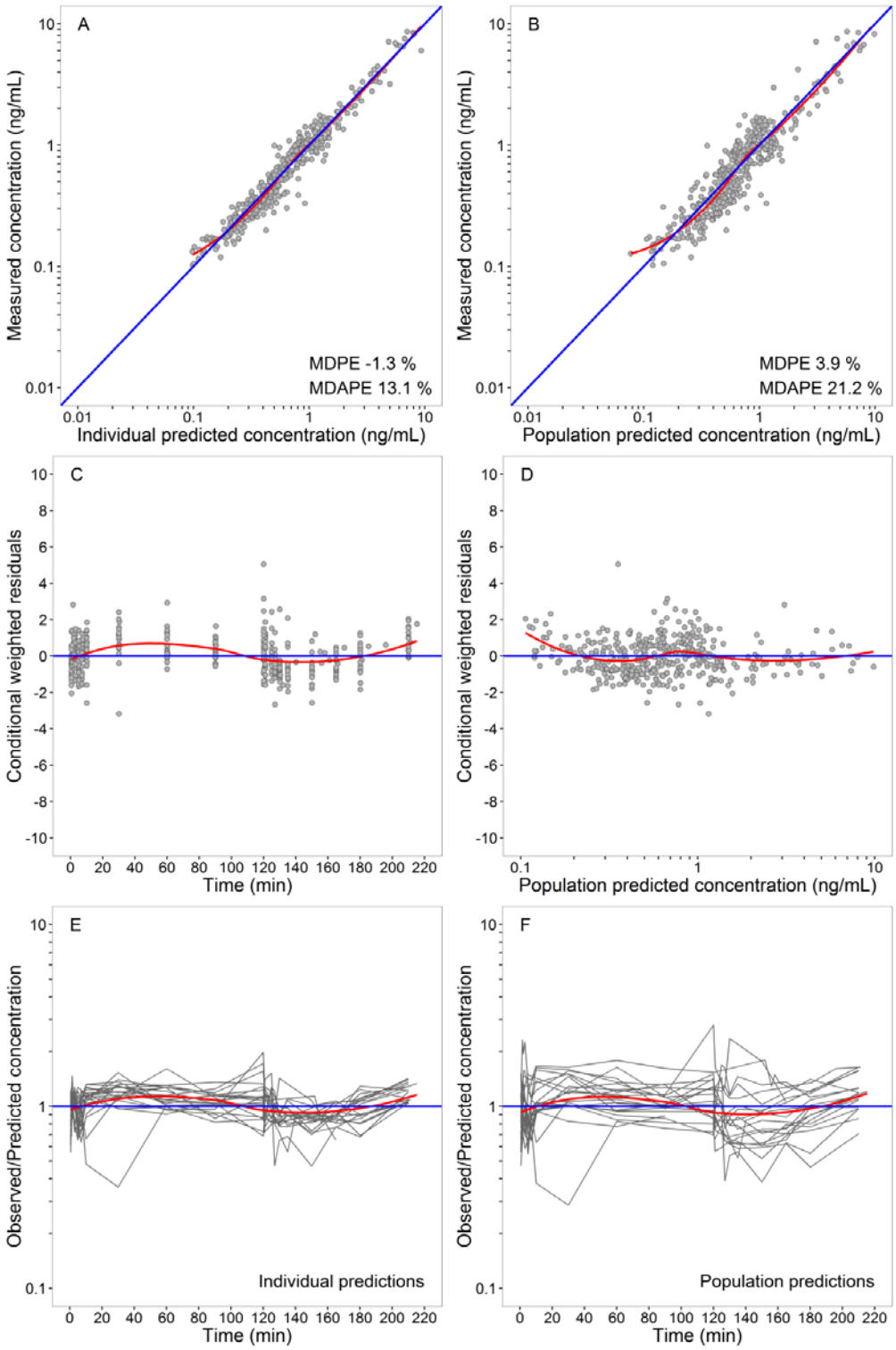

Figure S3: Goodness-of-fit plots for the final model of sufentanil plasma concentrations: measured concentrations versus individual Bayesian predictions (A) and versus population predictions (B); conditional weighted residuals vs. time (C) and vs. population predicted concentrations (D); ratio of measured to predicted concentrations vs. time for the individual (E) and the population predictions (F). The blue lines represent the lines of identity (measured = predicted). The red lines are smoothing lines through the data as obtained by locally weighted regression. MDPE, median prediction error; MDAPE, median absolute prediction error.

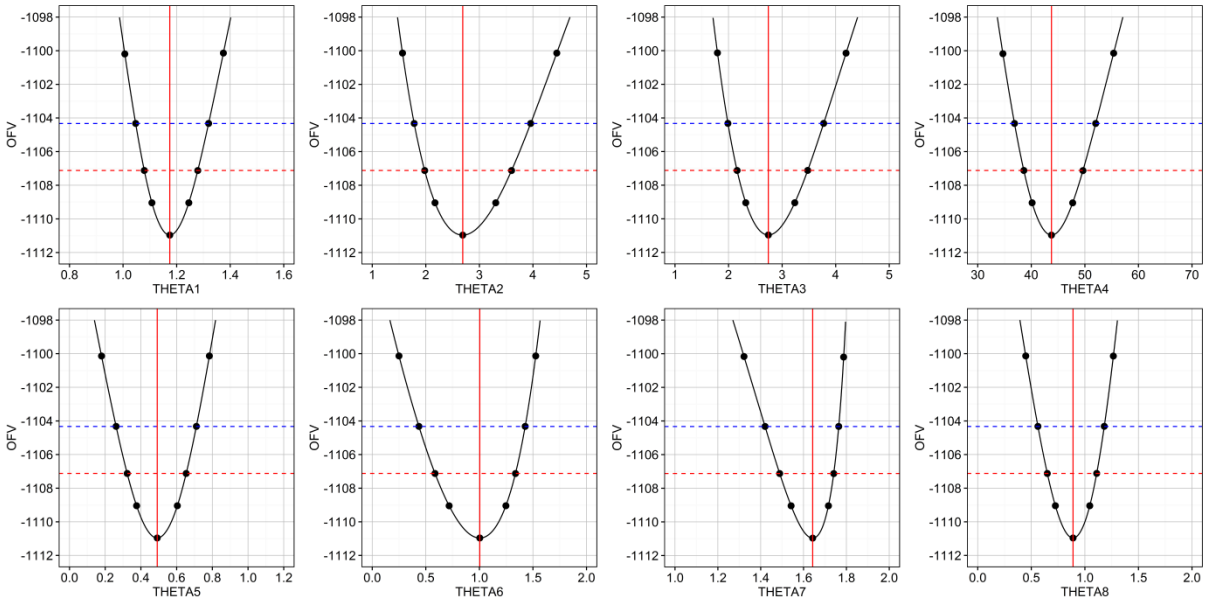

Figure S4: Log-likelihood profiles of the pharmacokinetic parameters. Critical values of the objective function value are shown as red and blue dotted line for $p<0.05$ and $p<0.01$, respectively. The vertical red line marks the population estimate of the parameter. OFV, objective function value.

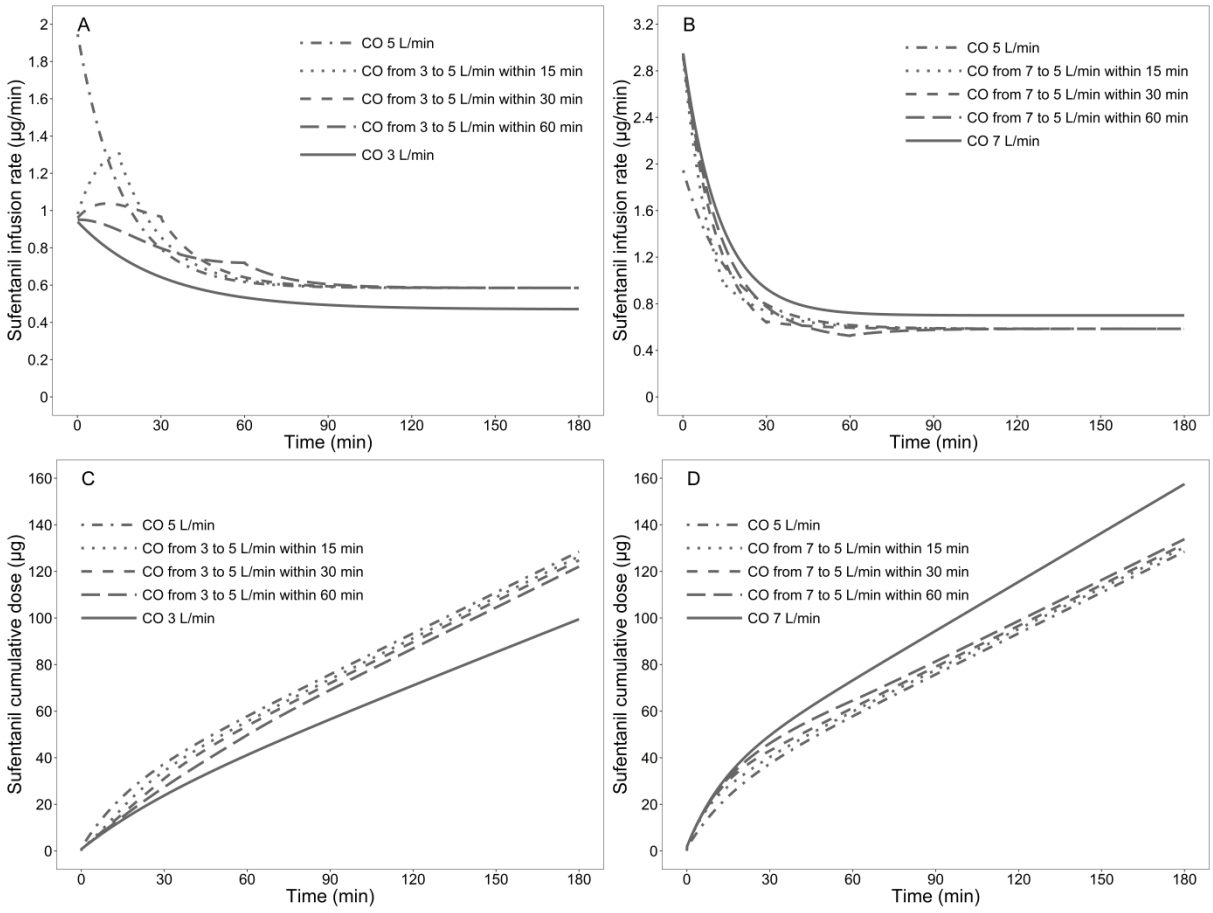

Figure S5: Sufentanil infusion rates needed to maintain a constant sufentanil plasma concentration of 0.5 ng · ml^{-1} for 3 h during restoration of normal cardiac output after start of sufentanil infusion (A and B), and the corresponding cumulative sufentanil doses associated with these infusion rates (C and D). CO, cardiac output.

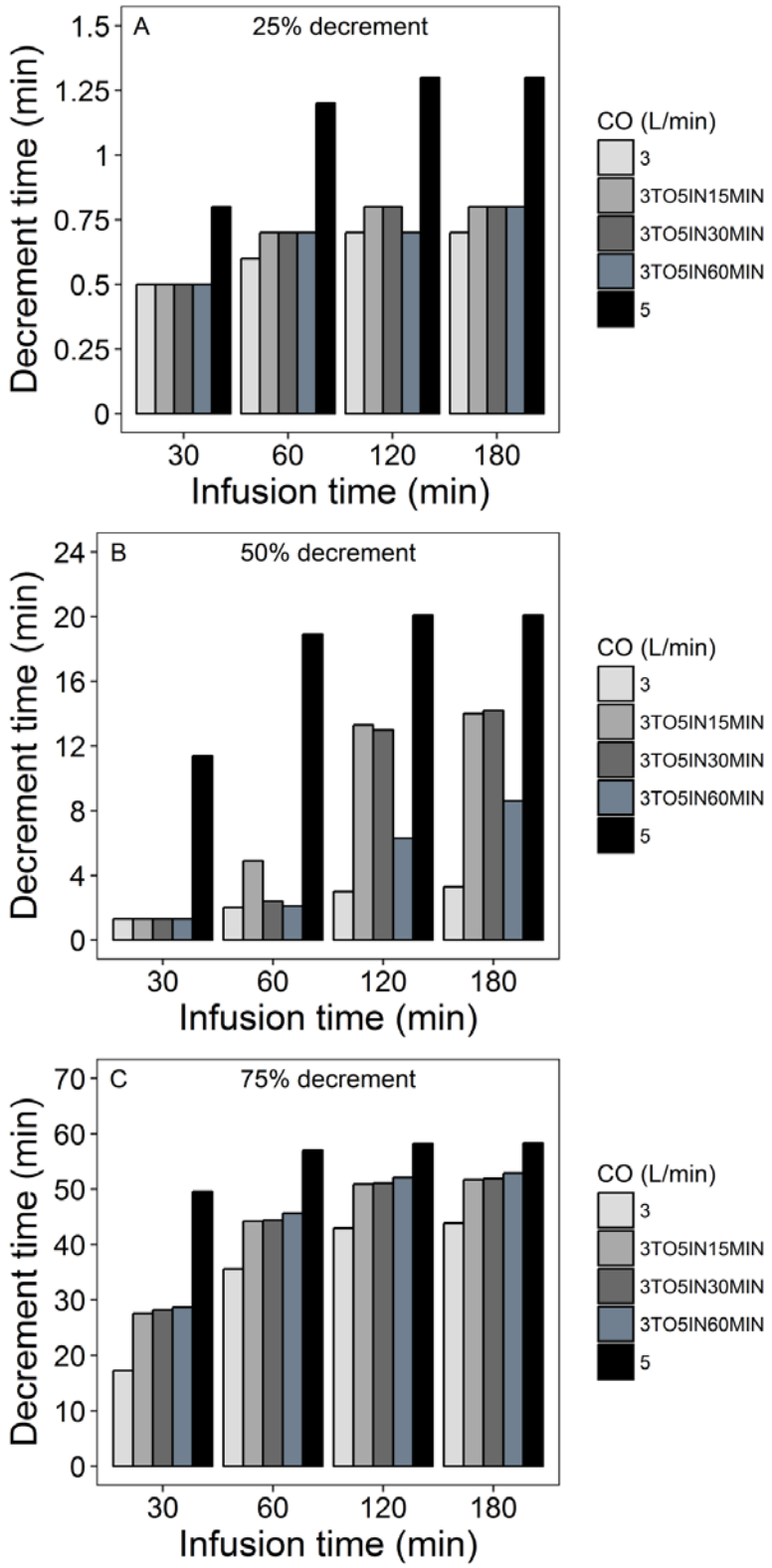

Figure S6: Time required for 25% (A), 50% (B), and 75% (C) decrease in plasma concentration of sufentanil after a continuous infusion of variable length. After stop of sufentanil infusion, the cardiac output was maintained constant at 3 or 5 $L \cdot min^{-1}$, or it was linearly increased from 3 to 5 $L \cdot min^{-1}$ during different periods of time. CO, cardiac output; 3TO5IN15MIN, cardiac output increase during 15 min; 3TO5IN30MIN, cardiac output increase during 30 min; 3TO5IN60MIN, cardiac output increase during 60 min.

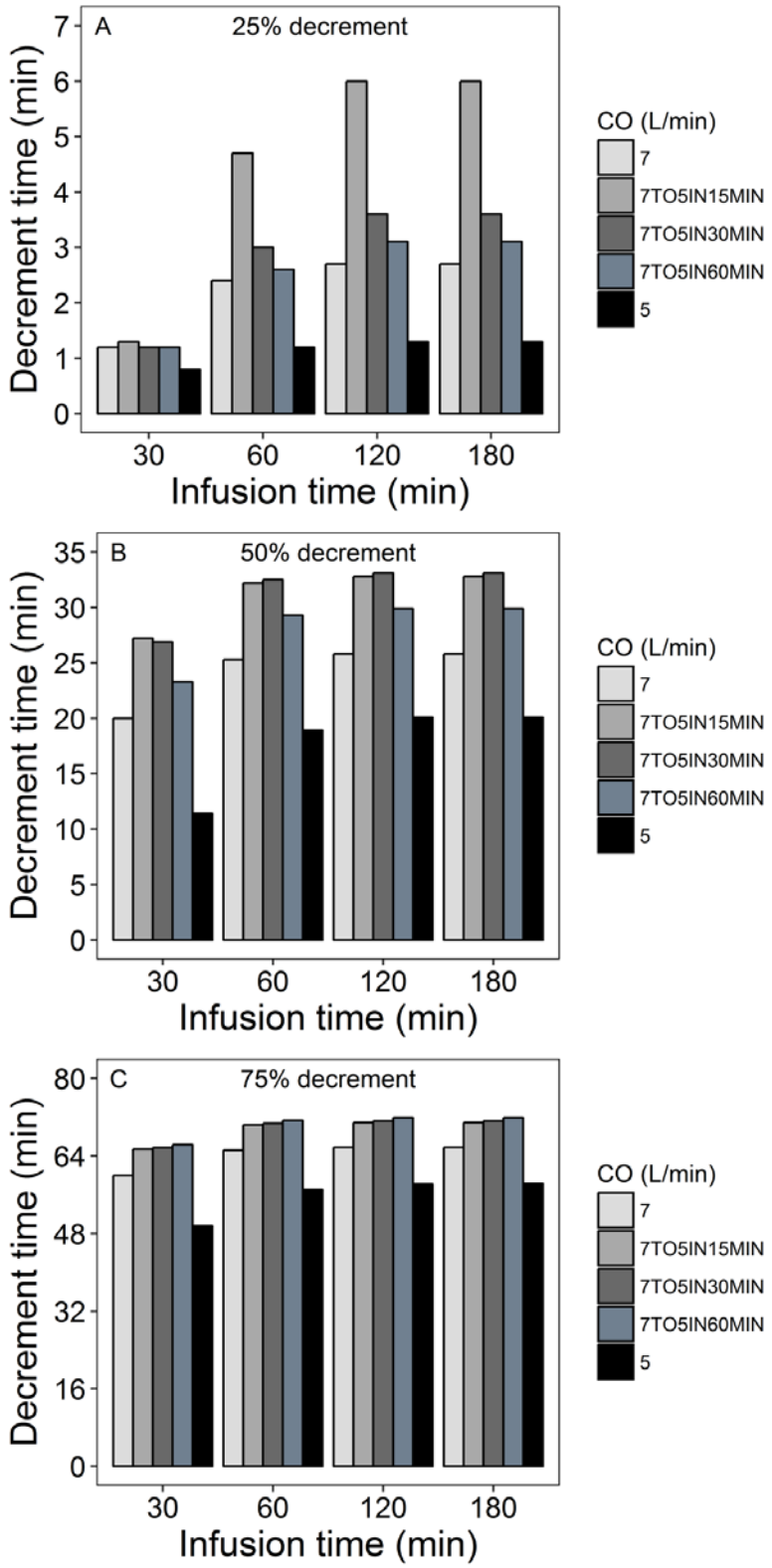

Figure S7: Time required for 25% (A), 50% (B), and 75% (C) decrease in plasma concentration of sufentanil after a continuous infusion of variable length. After stop of sufentanil infusion, the cardiac output was maintained constant at 7 or 5 $L \cdot min^{-1}$, or it was linearly decreased from 7 to 5 $L \cdot min^{-1}$ during different periods of time. CO, cardiac output; 7TO5IN15MIN, cardiac output decrease during 15 min; 7TO5IN30MIN, cardiac output decrease during 30 min; 7TO5IN60MIN, cardiac output decrease during 60 min.

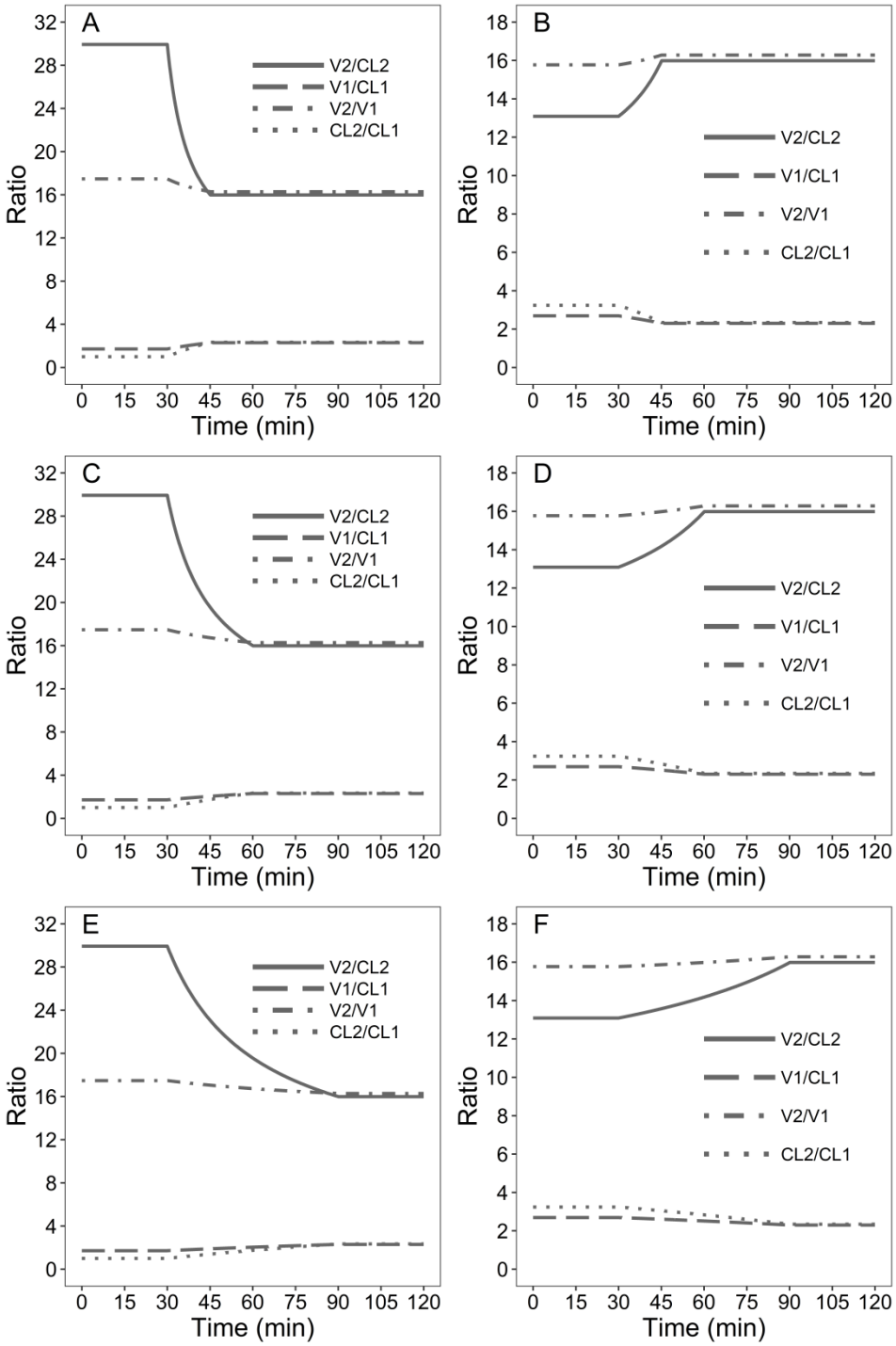

Figure S8: Changes in ratios of distribution volumes and clearances as induced by cardiac output changes after a target controlled infusion of sufentanil with a plasma concentration of 0.5 ng·mL^{-1} for 30 min. The cardiac output was linearly increased from 3 to 5 L·min^{-1} (A, C, E) or linearly decreased from 7 to 5 L·min^{-1} (B, D, F). The cardiac output changes were simulated as within 15 (A, B), 30 (C, D), and 60 min (E, F) after stop of sufentanil infusion. V2/CL2, equilibration time between peripheral and central compartment; V1/CL1, elimination time; V2/V1, ratio of volumes of distributions; CL2/CL1, ratio of clearances.